Suberin plasticity to developmental and exogenous cues is regulated by a set of MYB transcription factors

Vinay Shukla[a], Jian-Pu Han[a], Fabienne Cléard[a], Linnka Lefebvre-Legendre[a], Kay Gully[b], Paulina Flis[c], Alice Berhin[b,1], Tonni G. Andersen[b,2], David E. Salt[c], Christiane Nawrath[b], and Marie Barberon[a,3]

[a]Department of Botany and Plant Biology, University of Geneva, 1211 Geneva, Switzerland; [b]Department of Molecular Plant Biology, University of Lausanne, 1015 Lausanne, Switzerland; and [c]Future Food Beacon of Excellence and School of Biosciences, University of Nottingham, NG7 2RD Nottingham, United Kingdom

Edited by Julia Bailey-Serres, University of California, Riverside, CA, and approved August 22, 2021 (received for review January 28, 2021)

Suberin is a hydrophobic biopolymer that can be deposited at the periphery of cells, forming protective barriers against biotic and abiotic stress. In roots, suberin forms lamellae at the periphery of endodermal cells where it plays crucial roles in the control of water and mineral transport. Suberin formation is highly regulated by developmental and environmental cues. However, the mechanisms controlling its spatiotemporal regulation are poorly understood. Here, we show that endodermal suberin is regulated independently by developmental and exogenous signals to fine-tune suberin deposition in roots. We found a set of four MYB transcription factors (MYB41, MYB53, MYB92, and MYB93), each of which is individually regulated by these two signals and is sufficient to promote endodermal suberin. Mutation of these four transcription factors simultaneously through genome editing leads to a dramatic reduction in suberin formation in response to both developmental and environmental signals. Most suberin mutants analyzed at physiological levels are also affected in another endodermal barrier made of lignin (Casparian strips) through a compensatory mechanism. Through the functional analysis of these four MYBs, we generated plants allowing unbiased investigation of endodermal suberin function, without accounting for confounding effects due to Casparian strip defects, and were able to unravel specific roles of suberin in nutrient homeostasis.

root | suberin | endodermis | ABA | CIF

Plant roots form an inverted epithelium responsible for the selective acquisition of water and nutrients present in the soil. When entering the root, water and nutrients need to be radially transported from the root periphery to the central vasculature in order to be loaded to the xylem vessels and distributed to the plant organs. This can be achieved through three different transport scenarios: symplastic, apoplastic, or transcellular (1, 2). The endodermis, the innermost cortical cell layer surrounding the central vasculature, plays a particularly important role in these transport routes as it forms barriers for the free diffusion of water and nutrients. These barriers are formed in two sequential differentiation stages with first, the formation of Casparian strips (CSs), ring-like structures made of lignin forming an apoplastic barrier (3–5), and then suberin lamellae deposited as secondary cell walls around endodermal cells, forming a diffusion barrier for the transcellular pathway (5–7). Recent efforts studying mutants and lines affected for CSs and/or endodermal suberin in *Arabidopsis thaliana* and in rice demonstrated that both barriers play crucial roles in nutrient acquisition and homeostasis (6, 8–13). Yet, the role of suberin in nutrient transport is still poorly understood and, in the absence of mutants with a constitutive, strong reduction in suberization, is mainly corroborated by the analysis of a synthetic suberin-deficient line (artificially expressing in the endodermis the cutinase CDEF1, CUTICLE DESTRUCTING FACTOR1, to degrade suberin) (6, 11, 14). To complicate matters, most known enhanced suberin mutants are actually Casparian strip defective mutants, with ectopic endodermal lignification and suberization acting as compensation (9–11). This syndrome occurs in response to Casparian strip defects and is triggered through the endodermal integrity control system consisting of the leucine-rich-repeat receptor-like kinase, SGN3/GSO1 (SCHENGEN3/GASSHO1) and its ligands CIF1/2 (CASPARIAN STRIP INTEGRITY FACTORS 1/2) (12, 15–19). Suberin, however, is not only regulated by endogenous developmental factors surveilling Casparian strip integrity. Pointing toward a very central role of suberin in plants' adaptation to their environment, endodermal suberization is also highly regulated by nutrient availability and the hormones ethylene and abscisic acid (ABA) (6, 14, 20–25), as well as during biotic interactions (25–28). How suberin is regulated in response to developmental and exogenous clues remains poorly understood. Recently, several transcription factors were shown to be sufficient to induce ectopic suberin formation when ectopically overexpressed and for some to directly activate the expression of suberin biosynthesis genes (29–33). Suggesting a potential role in controlling endodermal suberization the transcription factors *MYB39*, *MYB93* (*MYeloBlastosis* family of transcription factors), and *ANAC046* (*A. thaliana NAM/ATAF/CUC protein*) were shown to be constitutively expressed in the endodermis and *MYB41* to be expressed in the endodermis in response to ABA or salt, two

Significance

Endodermal suberin plays crucial roles in plant nutrition by forming barriers for the free diffusion of water and nutrients. Suberin formation is tightly regulated by exogenous and developmental cues, which independently control suberin deposition in the endodermis. A set of four MYB transcription factors, expressed in the endodermis and responding to suberin-inducing conditions, individually prompt suberization and include the MYBs required for suberin formation and regulation. Overexpressing these transcription factors specifically in the endodermis or mutating all four led to plants specifically overproducing or underproducing endodermal suberin, respectively. Physiological analysis of these plants allowed us to decipher the role of suberin independently of synthetic transgenes and other endodermal barriers.

Author contributions: M.B. designed research; V.S., J.-P.H., F.C., L.L.-L., K.G., P.F., A.B., T.G.A., and M.B. performed research; V.S., F.C., L.L.-L., A.B., T.G.A., D.E.S., and C.N. contributed new reagents/analytic tools; V.S., J.-P.H., K.G., P.F., C.N., and M.B. analyzed data; D.E.S. provided ionomic expertise; and V.S. and M.B. wrote the paper.

The authors declare no competing interest.

This article is a PNAS Direct Submission.

[1]Present address: UCLouvain, Louvain Institute of Biomolecular Science and Technology, Université Catholique de Louvain, 1348 Louvain-la-Neuve, Belgium.

[2]Present address: MPI for Plant Breeding Research, Department for Plant-Microbe Interactions, 50829, Köln, Germany.

[3]To whom correspondence may be addressed. Email: marie.barberon@unige.ch.

This article contains supporting information online at https://www.pnas.org/lookup/suppl/doi:10.1073/pnas.2101730118/-/DCSupplemental.

Published September 22, 2021.

conditions known to induce suberization (29, 31, 32, 34). However, in the absence of clear suberin phenotypes associated with loss of function, their actual role in endodermal suberin formation and its regulation remains unclear.

Here by combining epistasis and pharmacological experiments, we demonstrated that suberin is regulated independently by the SGN3/CIFs pathway and ABA (previously shown to control suberin induction in response to nutritional stresses). We next undertook a systematic gene expression analysis and identified four endodermal MYB transcription factors (MYB41, MYB53, MYB92, and MYB93) acting downstream of SGN3/CIFs and ABA signaling, in the endodermis. These transcription factors are sufficient to induce suberin biosynthesis in the endodermis. Moreover, we generated a quadruple mutant by CRISPR-Cas9 and could show that several MYB transcription factors are necessary to form endodermal suberin and/or to induce suberization in response to developmental and exogenous signaling. Our work developed plants specifically and strongly impaired in endodermal suberin, allowing us not only to probe the regulatory mechanisms of suberin formation but also to characterize the function of suberin in nutrient homeostasis independently of Casparian strip defects.

Results

Suberin Is Induced by ABA and SGN3/CIFs Independently. Suberin formation can be induced in response to nutrient availability through ABA and in response to Casparian strip defects through the receptor SGN3/GSO1 and its ligands CIF1/2 (6, 12, 16, 17). In order to investigate the underlying molecular mechanism controlling ectopic suberization, it was important to establish whether ABA and SGN3/CIFs have a similar effect on suberin formation. We compared the effects of exogenous applications of the hormone ABA and the peptide CIF2 on root suberization. To this end we used the suberin biosynthesis reporter line *GPAT5::mCitrine-SYP122* (driving the expression of a fluorescently tagged plasma membrane anchor protein under the control of the promoter of the suberin biosynthesis gene *Glycerol-3-Phosphate Acyl Transferase5*) and whole-mount suberin staining using Fluorol Yellow (FY) (Fig. 1 *A*–*C*). In untreated roots, we observed a typical pattern of suberin formation (5, 6, 35) with a non-suberized zone (state I of endodermal differentiation with Casparian strips) followed by a suberizing zone where only patches of endodermal cells are suberized (patchy zone) and finally a fully suberized zone (Fig. 1 *A*–*C*). Exogenous treatments with ABA or CIF2 peptide led to ectopic suberin formation at the proximity of the root tip, without a patchy zone between non-suberized and fully suberized zones (Fig. 1 *A*–*C*) with ABA additionally inducing further suberization in the fully differentiated endodermis and in cortical cells, as described before (6). Both treatments had the same effect on the onset of endodermal suberization, which begs the question of whether these two signals are converging on the same mechanism. This has been addressed before and independent work on this suggests either an interaction between ABA and developmental signals (36), or, on the contrary, an independence (14). In light of these contradictions, we decided to clarify the relation between ABA and SGN/CIFs as signals controlling endodermal suberization. We first tested whether the CIF1/2 receptor SGN3/GSO1 was needed for ABA-dependent suberization. We used the CIF-insensitive mutant *sgn3* and observed no difference between ABA-induced ectopic endodermal suberization in WT plants and in *sgn3* mutants (Fig. 1 *C* and *D*). This hints at ABA signaling being active either downstream or independent of the SGN3/CIFs pathway. To elucidate this further, we assessed whether exogenous CIF2 application can induce suberization in the absence of active ABA signaling. We used the previously described *ELTP::abi1-1* line, where ABA signaling is inhibited in the endodermis by expressing the dominant-negative *abi1-1* (*aba insensitive 1*) allele specifically in the endodermis using the *ELTP/EDA4* promoter (*Endodermal Lipid Transfer Protein/EMBRYO SAC DEVELOPMENT ARREST 4*) (6). As previously reported for *ELTP::abi1-1* plants, endodermal suberization was severely delayed in nonstressed conditions (6, 35), but CIF2 application was able to induce suberin formation similarly to the response observed in wild-type (WT) plants (Fig. 1*E*). This indicates that ABA signaling is not acting downstream of SGN3/CIFs and that both pathways control suberization independently. To strengthen this conclusion, we tested the role of ABA signaling in the SGN3/CIFs-dependent enhanced suberin phenotype observed in the Casparian strip defective mutant *esb1* (*enhanced suberin 1*) (9, 12). We first expressed *ELTP::abi1-1* in *esb1* mutant background and observed an enhanced suberin phenotype independent of endodermal ABA signaling (*SI Appendix*, Fig. S1*A*), confirming previous analysis (14). Next, we confirmed this observation by pharmacological interference with ABA biosynthesis using fluridone (an herbicide blocking the carotenoid biosynthesis indirectly and thus lowering the amount of ABA), widely used as an ABA biosynthesis inhibitor (37–39). In the presence of fluridone, suberin is highly reduced in WT plants but the *esb1* mutant still displays its enhanced suberin phenotype (*SI Appendix*, Fig. S1*B*). Altogether these data demonstrate that ABA and SGN3/CIFs pathways can induce ectopic endodermal suberization independently.

MYB41 Is a Primary Response Factor to Suberin-Inducing Signals. Next, we focused on identifying transcription factors controlling endodermal suberization downstream of ABA and SGN3/CIFs. Several MYB transcription factors—MYB9, MYB39, MYB41, MYB53, MYB92, MYB93, and MYB107—have been shown in transient assays in *Nicotiana benthamiana* leaves, ectopic overexpression in whole plant, and/or yeast one-hybrid experiments, to be able to activate suberin biosynthesis (29–33). Among them, MYB9 and MYB107 were shown to control suberin deposition in seed coats (40, 41). Very recently, MYB39 has been proposed as a regulator of endodermal suberization (31). However, the *myb39* mutant showed only a partial delay in endodermal suberization, suggesting the involvement of other transcriptional regulators. Moreover, the primary factors regulating suberin biosynthesis in response to exogenous and developmental cues were still unknown. To identify such factors, we narrowed our search to the *MYB*s whose expression was induced by both ABA and SGN3/CIFs pathways. We mined publicly available transcriptomes in seedlings treated with ABA for 1 h and 3 h (42) and roots treated with CIF2 peptide for 2 h and 8 h (17) and found a moderate response of all the selected *MYB*s (i.e., *MYB39*, *-53*, *-92*, and *-93*), with the exception of *MYB41* whose expression responded the fastest and strongest to either stimuli (*SI Appendix*, Fig. S2*A*). To validate this observation, we performed a time-course experiment for transcript profiling of roots after 3 h and 6 h of ABA or CIF2 applications in our growth conditions (Fig. 2*A*). We confirmed that *MYB41* was indeed the primary responsive factor for either stimuli. The other factors *MYB53*, *MYB92*, and *MYB93* were also induced by both stimuli in 3 to 6 h but at a lower levels, while *MYB39* expression was not significantly changed or reduced after ABA and CIF2 applications in our conditions after short (3 or 6 h) or longer treatment (12 or 24 h) and was therefore not investigated further in this study (Fig. 2*A* and *SI Appendix*, Fig. S2*B*).

Since *MYB41* reacted most prominently of all *MYBs* from transcript profiling, we focused on this factor as the primary candidate for controlling endodermal suberization and its induction by ABA and SGN3/CIFs. To test the spatiotemporal response of *MYB41* upon ABA and CIF2 applications, we developed a transcriptional reporter line, *MYB41::NLS-3xmVenus* for live imaging in roots. We found that *MYB41* was specifically expressed in the differentiated endodermis, matching the tissue specificity of the suberin biosynthesis reporter *GPAT5* (Fig. 2*B*). Applications of ABA and CIF2 further validated the transcriptional response observed in previous experiments of mRNA profiling as we observed a strong activation of *MYB41* promoter activity in the

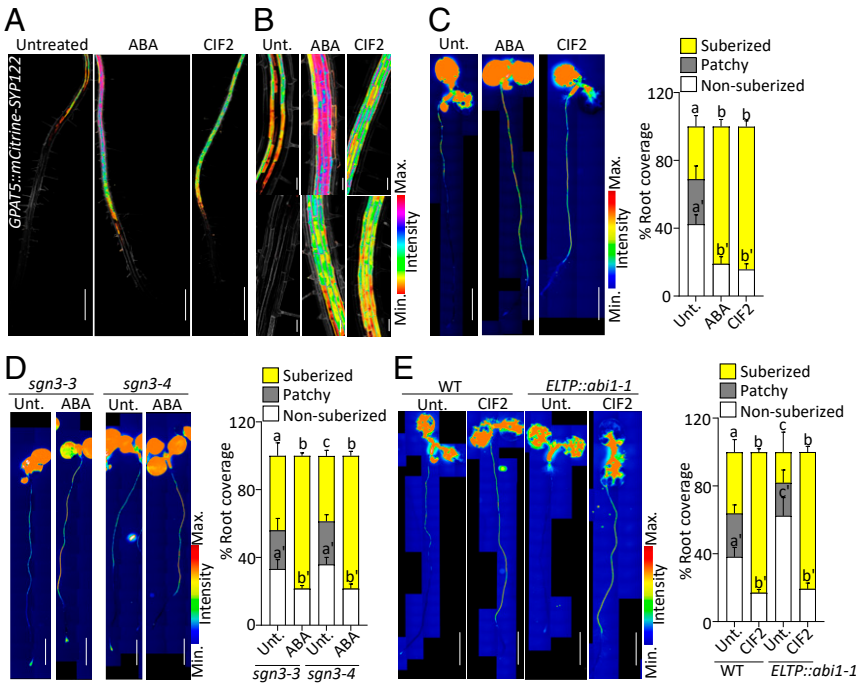

Fig. 1. Independent suberin induction by ABA and SGN3/CIF. (*A* and *B*) *GPAT5::mCITRINE-SYP122* expression (presented as Look Up Table, [LUT]) in untreated (Unt.) or plants treated with 1 μM ABA or 1 μM CIF2 for 16 h. Propidium iodide (PI, in gray) was used to highlight cells. Pictures are presented as maximum intensity Z projections. (*A*) Observations from root tip to 4 to 5 mm. (Scale bars, 500 μm.) (*B*) Zoomed pictures from *A* in the patchy (*Upper*) and nonsuberized zones (*Lower*), respectively. (Scale bars, 50 μm.) (*C*–*E*) FY staining for suberin. Whole-mount staining in full seedlings (*Left*) and quantifications of suberin pattern along the root (*Right*), $n \geq 10$, error bars, SD, different letters indicate significant differences between conditions ($P < 0.05$). (Scale bars, 2 mm.) (*C*) FY staining for suberin in Unt. or treated WT plants with 1 μM ABA or 1 μM CIF2 for 16 h. (*D*) FY staining in *sgn3-3* and *sgn3-4* mutants Unt. or treated with 1 μM ABA for 16 h. (*E*) FY staining for WT and *ELTP::abi1-1* Unt. or treated with 1 μM CIF2 for 16 h.

endodermis with an ectopic expression close to the root tip (*SI Appendix*, Fig. S2 *C* and *D*). We combined this reporter with *GPAT5::NLS-3xmScarlet-I* to generate a dual reporter for *MYB41* and *GPAT5* promoter activity and observed in untreated conditions, that *MYB41* expression preceded the expression of *GPAT5* in the endodermis, positioning *MYB41* in a spatiotemporal context for regulating endodermal suberization (Fig. 2*C*). Upon ABA and CIF2 applications, *MYB41* expression was strongly induced, and its expression pattern extended to the proximity of the root tip. Since *MYB41* expression always preceded *GPAT5* spatiotemporal expression (Fig. 2*C* and *SI Appendix*, Fig. S2 *E* and *G*), this could be indicative of *MYB41* controlling the suberin biosynthesis machinery in the endodermis.

We then tested whether MYB41 activity was sufficient to induce endodermal suberization. To this end, we used the endodermis-specific promoter *CASP1* (expressed in the differentiating endodermis before suberization) to drive *MYB41* expression. FY staining of *CASP1::MYB41* transgenic lines showed ectopic endodermal suberization closer to the root tip, demonstrating that *MYB41* expression was sufficient for induction of endodermal suberization (Fig. 2*D*). We confirmed this observation by performing chemical analysis of suberin content in the roots of WT and two independent *CASP1::MYB41* lines. We found that both *CASP1::MYB41* lines displayed excess of suberin monomers with an increase of ~140% for line #3 and ~170% for line #7 compared with WT roots (Fig. 2*E*). We simultaneously tested the same by expressing a functional *MYB41-mVenus* under a chemically inducible endodermal promoter, *CASP1xve* in WT (*SI Appendix*, Fig. S2*H*) and *GPAT5::NLS-RFP* reporter backgrounds. Importantly after estradiol induction, we could observe a transient accumulation of MYB41-mVenus in endodermal cells followed by the induction of *GPAT5* promoter activity, corroborating our supposition that MYB41 can induce suberin biosynthesis in the endodermis (Fig. 2*F* and *SI Appendix*, Fig. S2 *I* and *J*). In order to verify whether this conditional induction of MYB41 was able to induce the rest of the suberin biosynthetic pathway, we measured the transcript levels of suberin biosynthesis genes and the other *MYB*s of interest. A short treatment of 3 h with estradiol was enough to strongly induce *MYB41* expression as well as nearly all the genes involved in suberin biosynthesis, including the recently characterized *GELPs* (*GDSL-Type Esterase/Lipases*) (43) coding for enzymes involved in the polymerization of suberin monomers in the cell wall (Fig. 2*G*). Surprisingly we could also observe an increased expression for *ASFT*, *PAL1*, *PAL2*, *PAL4*, and *C4H* while no significant increase in ferulate content was detected (Fig. 2 *E* and *G*). In addition, we observed that MYB41 did not induce the expression of most other *MYB*s studied with only a transient induction of *MYB93* expression and a reduction of the expression of *MYB39*, *MYB53*, and *MYB92* after 6 h of estradiol induction (Fig. 2*G*). This reduction of *MYB39*, *MYB53*, and *MYB92* expression, being observed only after 6 h while the expression of genes involved in suberin biosynthesis was already induced after 3 h, likely reflects a compensatory effect.

A Set of Four MYBs Controls Suberin Biosynthesis and Regulation. After establishing that MYB41 was sufficient to induce endodermal suberization, we wondered whether it was also required to establish the endodermal suberin pattern observed under unstressed conditions in wild-type plants. We generated two CRISPR alleles of *MYB41*: *myb41_c1*, obtained by a nearly full deletion of the *MYB41* coding region, and *myb41_c2*, obtained by introducing a one-base pair frame shift in the beginning of the third and longest exon of *MYB41* gene (*SI Appendix*, Fig. S3*A*). To confirm the protein inactivity from the point mutation generated in *myb41_c2*, the mutated *MYB41_c2* complementary DNA (cDNA) was cloned and expressed in plants using the *CASP1* promoter and, unlike the

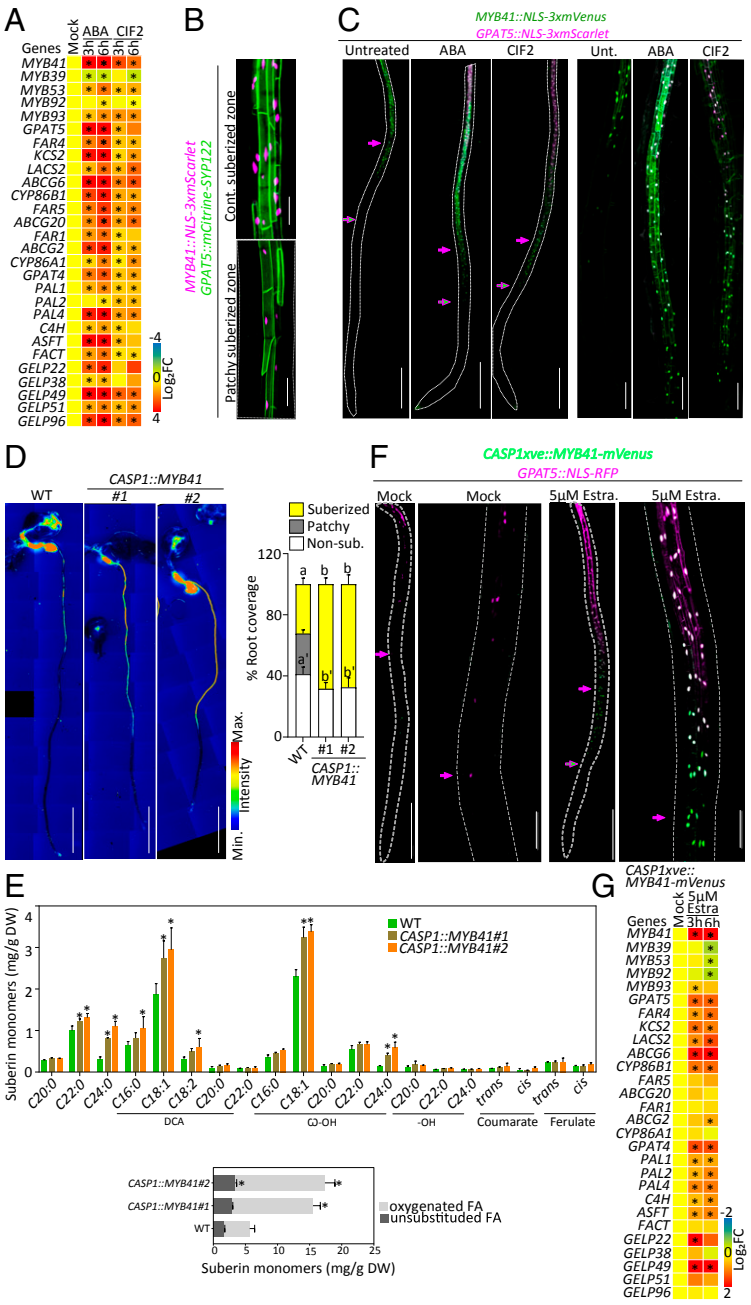

Fig. 2. MYB41, an endodermal transcription factor, inducing suberin biosynthesis. (*A*) Relative expression levels of the candidate *MYBs* and suberin biosynthesis and polymerization genes in WT roots treated with 1 µM ABA or 1 µM CIF2 for 3 and 6 h ($n = 4$ pools of 25 to 30 roots). Results are presented as fold changes compared with the mock condition. Numeric values are presented in *SI Appendix*, Table S3. Asterisks indicate statistically significant differences ($P < 0.05$). (*B*) Dual reporter for *GPAT5::mCitrine-SYP122* and *MYB41::NLS-3xmScarlet* under untreated condition. Pictures are presented as maximum intensity Z projections taken in the zone of continuous suberization (*Upper*) and patchy suberization (*Lower*). (Scale bars, 50 µm.) (*C*) Dual reporter for *GPAT5::NLS-3xmScarlet* and *MYB41::NLS-3xmVenus* upon 16-h treatments with 1 µM ABA or 1 µM CIF2. Pictures are presented as maximum intensity Z projections from the root tip to 4 to 5 mm (*Left*) and zoomed views (*Right*) corresponding to the zone prior to suberization in untreated conditions. Arrows highlight the onset of *MYB41* (green) and *GPAT5* (magenta) expression. (Scale bars, 500 µm.) Quantifications are shown in *SI Appendix*, Fig. S2*D*. (*D*) FY staining of WT and two independent *CASP1::MYB41* lines. Whole-mount staining (*Left*) and quantifications of suberin pattern are presented (*Right*), $n \geq 10$, error bars, SD, different letters indicate significant differences between conditions ($P < 0.05$). (Scale bars, 2 mm.) (*E*) Polyester composition in 5-d-old roots of WT and two independent *CASP1::MYB41* lines. Individual suberin monomer content (*Upper*) and the corresponding total amount of unsubstituted and oxygenated fatty acids (*Lower*) are presented. Data correspond to mean; error bars, SD ($n = 4$ pools of 200 to 300 roots). FA, fatty acid; DCA, dicarboxylic fatty acid; ω-OH, ω-hydroxy fatty acid; DW, dry weight. Asterisks represent statistical significant differences compared with WT ($P < 0.05$). Results from WT are also shown in Fig. 4*B*. (*F*) *CASP1xve::MYB41-mVenus* in *GPAT5::NLS-RFP* background for mock and 5 µM estradiol (Estra.) treatment for 16 h . Pictures are presented as Z projections from the root tip to 4 to 5 mm (*Left*) and zoomed views (*Right*) taken in the corresponding zone for patchy suberization in mock conditions. Arrows highlight the onset of *MYB41* (green) and *GPAT5* (magenta) expressions. (Scale bars, 500 µm [*Left*] and 100 µm [*Right*].) Quantifications are shown in *SI Appendix*, Fig. S2 *H* and *I*. (*G*) Relative expression levels of the *MYBs* candidates and suberin biosynthesis and polymerization genes in the roots of *CASP1xve::MYB41-mVenus* treated with 5 µM estradiol for 3 and 6 h ($n = 4$ pools of 25 to 30 roots). Results are presented as fold changes compared with the mock condition. Numeric values are presented in *SI Appendix*, Table S3. Asterisks indicate statistically significant differences ($P < 0.05$).

unmutated MYB41 cDNA, was unable to induce suberization (*SI Appendix*, Fig. S3*B*). Unexpectedly, FY staining showed that suberin deposition in the endodermis was unaffected in these two CRISPR mutants (Fig. 3*A*). Moreover, ABA or CIF2 treatment induced ectopic suberization in *myb41_c1* and *myb41_c2* mutants virtually indistinguishable from WT plants (Fig. 3*A*). These observations led us to consider that though *MYB41* was the primary responsive factor to ABA and CIF2 and is sufficient to induce suberization, other functionally redundant MYBs are probably compensating in its absence.

To identify other MYBs that might be active in the *myb41* mutants, we compared the transcript levels of the other *MYB* candidates in WT and *myb41_c1* mutant backgrounds and found that the mRNA levels of *MYB39*, *MYB53*, *MYB92*, and *MYB93* were slightly higher in *myb41_c1* compared with the WT in untreated conditions (*SI Appendix*, Fig. S3*C*). Upon ABA and CIF applications, all the *MYB*s except *MYB39*, were further induced in both backgrounds. Therefore, we decided to additionally characterize *MYB53*, *MYB92*, and *MYB93* in endodermal suberization. Similarly to MYB41, the selected MYB candidates, MYB53, MYB92, and MYB93, are able to induce ectopic endodermal suberization. FY staining of the lines *CASP1::MYB53*, *CASP1::MYB92*, and *CASP1::MYB93* along with *CASP1::MYB41*, clearly showed that endodermis-specific precocious expression of any of these *MYB*s was sufficient to induce suberization close to the root tip similarly to *MYB41* (Fig. 3*B*). Next, we wondered which one of these *MYB*s was expressed in the endodermis and generated promoter–reporter lines for *MYB53*, *MYB92*, and *MYB93* driving the expression of *NLS-3xmVenus*. We found that, similarly to *MYB41*, *MYB53*, *MYB92*, and *MYB93* were also expressed in unstressed conditions in the endodermis with *MYB53* and *MYB92* expressed from the differentiated zone (Fig. 3 *C*–*E*). However, *MYB93* expression was observed only in a few cells, most likely in the endodermis above the lateral root primordia (Fig. 3*E*) as it was previously described (34). Additionally, *MYB53* and *MYB92* were also expressed in a few isolated cortical and epidermal cells in unstressed conditions (Fig. 3 *C* and *D*). Importantly, all these promoters promptly responded to ABA and CIF2 resulting in a higher expression, with the expression of *MYB93* extending to the endodermal cells close to the root tip as observed for *MYB41* (Fig. 3 *C* and *D* and *SI Appendix*, Fig. S3 *D*–*F*). Taken together, we concluded that not a single MYB, but rather a group of MYB transcription factors is likely controlling suberin biosynthesis and regulation in the endodermis. To test this hypothesis we first characterized with FY staining the pattern of suberin deposition in *myb53*, *myb92*, and *myb93* mutants in unstressed conditions and in response to ABA and CIF2 treatments (Fig. 3*F* and *SI Appendix*, Fig. S3*G*). While *myb53* and *myb93* displayed no suberin phenotype in all conditions tested (*SI Appendix*, Fig. S3*G*), *myb92* showed a significant delay in suberin deposition in unstressed conditions with suberin deposited later from the root tip and only as patches of suberized cells (Fig. 3*F*). However, even in the *myb92* mutant, ABA or CIF2 treatment induced ectopic suberization similarly to the effect observed in WT plants (Fig. 3*F*). We therefore decided to mutate all four *MYB*s simultaneously by using multiplexed CRISPR technology (44) introducing frame shifts leading to loss of function in *MYB53*, *MYB92*, and *MYB93* in the mutant background, *myb41_c2* (*SI Appendix*, Fig. S4 *A* and *B*). After FY staining of the resulting quadruple mutant, *myb41-myb53-myb92-myb93* (*quad-myb*), we observed nearly a total absence of suberin in roots (Fig. 4*A*). Importantly, suberin induction by ABA and CIF2 treatments was also severely compromised in the *quad-myb* mutant where almost no induction was observed after 3 or 6 h and only a weak effect was observed after 16 h (Fig. 4*A* and *SI Appendix*, Fig. S4*C*). We confirmed this observation by performing chemical analysis of the suberin content in the roots of the *quad-myb* mutant compared with WT roots and found a strong reduction of both aliphatic and aromatic monomers (Fig. 4*B*). Dicarboxylic acids and ω-hydroxy acids were nearly absent with ∼90% reductions, while reductions in fatty alcohols ranged from 20 to 80%. Ferulate was reduced by ∼80% and coumarate showed a ∼50% reduction compared with WT. On average, the *quad-myb* mutant showed an overall ∼78% decrease in suberin monomers compared with WT (Fig. 4*B*). We also quantified the mRNA levels of suberin biosynthesis and polymerization genes and found that most were accumulating at lower levels, especially the genes involved in the fatty acid pathway and polymerization (Fig. 4*C*). The expression of genes involved in the phenylpropanoid biosynthesis were also affected with *PAL2* and *PAL4* expressed at higher levels but without leading to an increase of aromatic suberin components (Fig. 4 *B* and *C*). These genes being also expressed at higher levels in *CASP1xve::MYB41* after estradiol induction, their change in expression (Fig. 2*G*) is not directly affected by changes in the *MYB*s expression. The expression of *FACT* (*FATTY ALCOHOL:CAFFEOYL-CoA CAFFEOYL TRANSFERASE*), involved in the synthesis of root waxes (45) was decreased in the *quad-myb* mutant (Fig. 4*C*) while increased after ABA and CIF2 applications (Fig. 2*A*) but not in *CASP1xve::MYB41* after estradiol induction (Fig. 2*G*). This might suggest that root waxes could also be affected in suberin-inducing conditions and that some of the *MYB*s studied here might be involved in this regulation. Altogether, the analysis of the *quad-myb* mutant strongly supports a central role of the transcription factors MYB41, MYB53, MYB92, and MYB93 in the control of suberin biosynthesis and its regulation by the two main signals inducing endodermal suberization.

MYB-Dependent Suberization Reveals Specific Roles of Suberin in Nutrient Homeostasis. Having identified a set of four MYB transcription factors playing a central role in controlling suberin biosynthesis and regulation, we set out to use these MYBs as tools to manipulate endodermal suberin specifically. Indeed, although suberin is known to play important roles for nutrient homeostasis we often cannot distinguish its role from Casparian strips. Previous efforts relied on mutants such as *esb1*, *casp1casp3*, or *myb36* with pleiotropic endodermal defects in Casparian strip formation (9, 10, 14). Here we generated *MYB41* overexpressing plants as potentially interesting tools to specifically enhance endodermal suberin in plants. To our surprise, plants overexpressing *MYB41* under the *CASP1* promoter displayed interrupted Casparian strips accompanied by a delay in the establishment of their apoplastic barrier (*SI Appendix*, Fig. S4 *D* and *E*) similar to the defects observed in *esb1* or *casp1casp3* mutants (9, 12). This may indicate that a precocious suberin formation (concomitant with Casparian strip formation) interferes with Casparian strip formation. Using the *ELTP* promoter, whose endodermal expression is much weaker than *CASP1* and is not affected by ABA and CIF2 (*SI Appendix*, Fig. S4 *F* and *G*), to trigger *MYB41* expression, we observed ectopic suberin formation close to the root tip in the corresponding plants (*SI Appendix*, Fig. S4*H*) yet, importantly, without affecting Casparian strips and the establishment of the apoplastic barrier (*SI Appendix*, Fig. S4 *D* and *E*). We therefore have now access to dominant genetic tools to either enhance suberin specifically (*ELTP::MYB41*) or together with Casparian strip defects (*CASP1::MYB41*). In parallel we have generated in this study a mutant, *quad-myb*, with a dramatic reduction of suberin with no Casparian strip defects and no delay in the establishment of the apoplastic barrier (*SI Appendix*, Fig. S4 *D* and *E*). We therefore studied and compared the suberin-only affected plants *ELTP::MYB41*, with the nonsuberized *quad-myb* mutant as well as with the suberin and Casparian strip–affected *CASP1::MYB41* in order to understand better the consequences of reduced or enhanced endodermal suberin, independent or coinciding with Casparian strip defects. All plants generated were carefully studied for their growth and development in plates and in soil conditions. The corresponding seedlings were indistinguishable at early stages

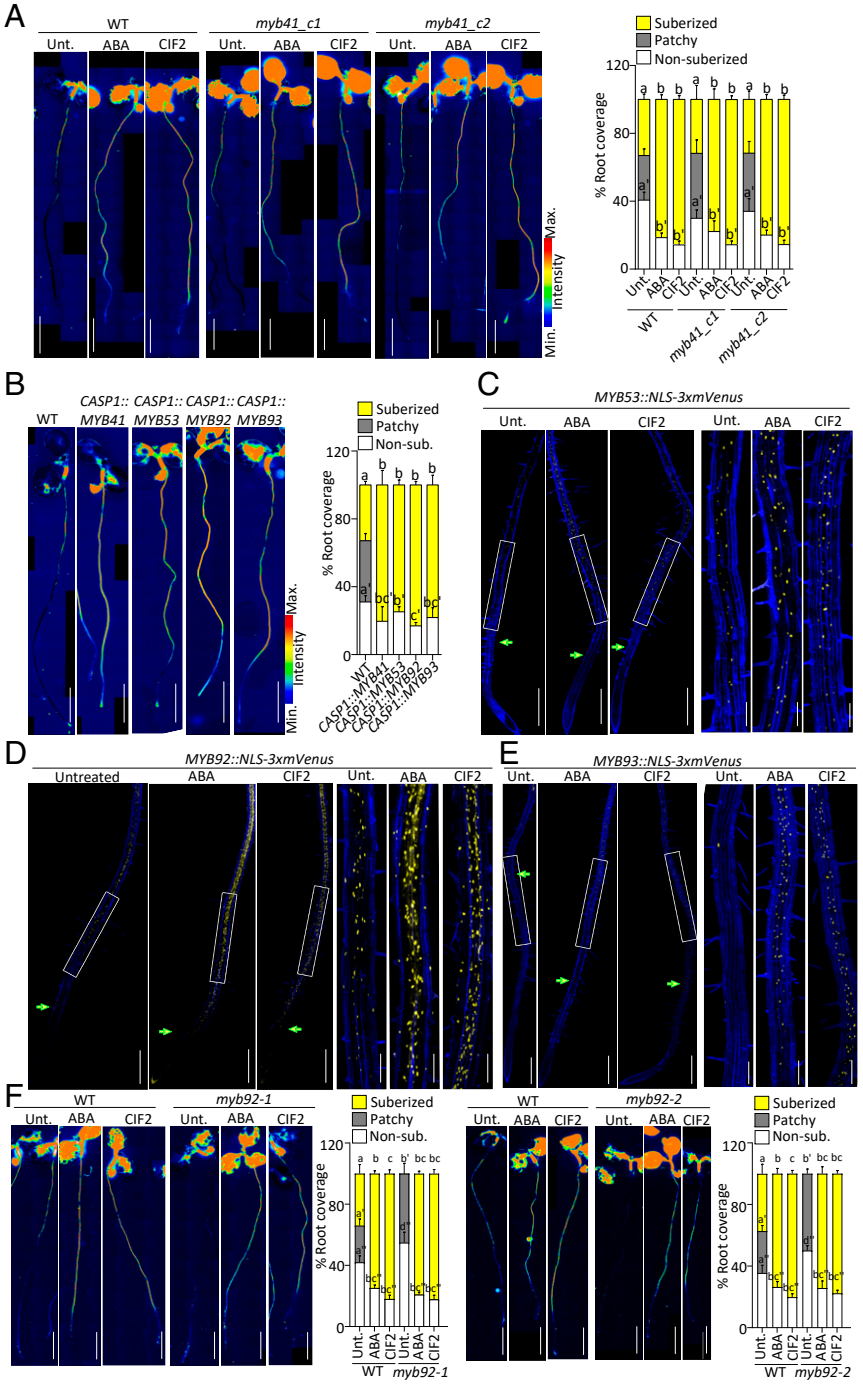

Fig. 3. *MYB53*, *MYB92*, and *MYB93* regulation and function in suberin induction. (*A*, *B*, and *F*) FY staining for suberin. Whole-mount staining (*Left*) and quantifications of suberin pattern along the root (*Right*), $n \geq 10$, error bars, SD. (Scale bars, 2 mm.) (*A*) FY staining of WT and two *myb41* CRISPR mutant alleles, *myb41_c1* and *myb41_c2* untreated or treated with 1 μM ABA or 1 μM CIF2 for 16 h. Different letters indicate significant differences between conditions for a given genotype ($P < 0.05$). (*B*) FY staining of WT, *CASP1::MYB41*, *CASP1::MYB53*, *CASP1::MYB92*, and *CASP1::MYB93* lines. Different letters indicate significant differences between conditions ($P < 0.05$). (*C*) *MYB53::NLS-3xmVenus*, (*D*) *MYB92::NLS-3xmVenus*, and (*E*) *MYB93::NLS-3xmVenus* expression (in yellow) untreated or after treatments with 1 μM ABA or 1 μM CIF2 for 16 h. (*C–E*) Pictures are presented as maximum intensity Z projections taken from the root tip to 4 to 5 mm (*Left*) with zoomed views corresponding to the zone of patchy suberization in untreated plants (*Right*). Arrows highlight the onset of expression. Propidium iodide (PI, in blue) was used to highlighted cells. (Scale bars, 500 μm [*Left*] and 125 μm [*Right*].) Quantifications are shown in *SI Appendix*, Fig. S3 *D–F*. (*F*) FY staining of WT, and *myb92* mutants untreated or treated with 1 μM ABA or 1 μM CIF2 for 16 h. Different letters indicate significant differences between conditions for a given genotype ($P < 0.05$).

of development in terms of growth, root length, or root hair density, where most of histological, chemical, expression and ionomic analysis were performed (*SI Appendix*, Fig. S5 *C* and *D*). At later stages we observed minor changes in primary root length, although the number and length of lateral roots was highly reduced in both *ELTP::MYB41* and *CASP1::MYB41* lines and increased in the *ELTP::CDEF1* line (*SI Appendix*, Fig. S5*A*). The *quad-myb* mutant was slightly affected in primary root length but not for lateral roots

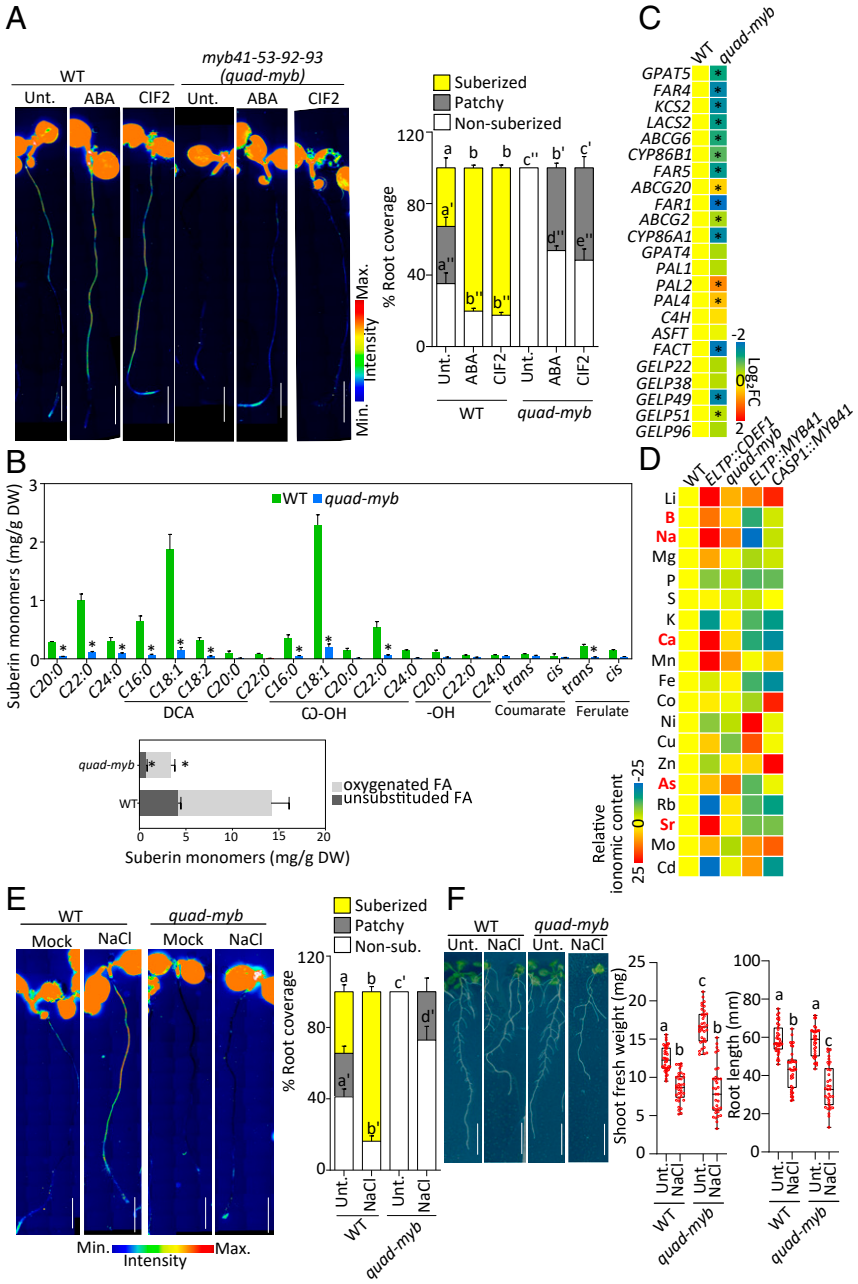

Fig. 4. Impaired suberin formation and regulation in quad-myb mutant associated with nutritional changes. (*A* and *E*) FY staining for suberin. Whole-mount staining (*Left*) and quantifications of suberin pattern along the root (*Right*), $n \geq 10$, error bars, SD, different letters indicate significant differences between conditions ($P < 0.05$). (Scale bars, 2 mm.) (*A*) FY staining of WT and *myb41-myb53-myb92-myb93* (*quad-myb*) mutant untreated or treated with 1 μM ABA or 1 μM CIF2 for 16 h. (*B*) Polyester composition in 5-d-old roots of WT and two independent *CASP1::MYB41* lines. Individual suberin monomer content (*Upper*) and the corresponding total amount of unsubstituted and oxygenated fatty acids (*Lower*) are presented. Data are represented as mean; error bars, SD ($n = 4$ pools of 200 to 300 roots). FA, fatty acid; DCA, dicarboxylic fatty acid; ω-OH, ω-hydroxy fatty acid; DW, dry weight. Asterisks represent statistically significant differences ($P < 0.05$). Results from WT are also shown in Fig. 2*E*. (*C*) Relative expression levels of the suberin biosynthesis and polymerization genes in the roots of *quad-myb* mutant compared with WT ($n = 4$ pools of 25 to 30 roots). Results are presented as fold changes compared with WT. Numeric values are presented in *SI Appendix*, Table S3. Asterisks indicate statistical significance ($P < 0.05$). (*D*) Ionomic profiling of leaves of WT, *ELTP::CDEF1*, *quad-myb*, *ELTP::MYB41*, and *CASP1::MYB41* plants. Elements were determined by ICP-MS. Results are presented as average fold changes compared with WT. Results from individual experiments are presented in *SI Appendix*, Fig. S5*E* and numeric values in *SI Appendix*, Table S4. (*E*) FY staining of WT and *quad-myb* mutant untreated or treated with 75 mM NaCl for 16 h. (*F*) NaCl effect on quad-myb root shoot weight and root length. WT and *quad-myb* plants were grown 3 d after which they were treated with 75 mM NaCl for next 10 d. Results are presented as pictures of plants at the end of day 13 (*Left*) and as quantifications (*Right*). Data are presented as box plots with individual values overlaid, $n \geq 30$, error bars, different letters indicate significant differences between conditions ($P < 0.05$). (Scale bars, 10 mm.)

in our conditions (*SI Appendix*, Fig. S5*A*). These changes in root architecture could be associated with enhanced or reduced suberization directly affecting root development, as it was previously suggested (11), or indirectly as a consequence of changes in nutrient acquisition. In soil, after 2 to 3 wk of growth we could observe that all genotypes were comparable (*SI Appendix*, Fig. S5*B*).

Therefore, manipulation of endodermal suberin had no dramatic consequences on plant growth and development allowing further physiological characterization of the corresponding plants.

To study the consequences of endodermal suberin manipulation for nutrient homeostasis, we performed inductively coupled plasma-mass spectrometry (ICP-MS) for elemental profiling in leaves (Fig. 4*D* and *SI Appendix*, Fig. S5*D* and Table S4). Confirming previous analysis in independent growth conditions (6), *ELTP::CDEF1* leaves accumulated arsenic, lithium, magnesium, and sodium at higher levels and potassium and rubidium at lower levels compared with WT plants. We observed additional ionomic changes in our growth conditions with a higher accumulation of boron, calcium, manganese, strontium, and molybdenum and a lower accumulation of phosphorous, iron, zinc, and cadmium in *ELTP::CDEF1* compared with WT. The *quad-myb* mutant also displayed multiple ionomic changes compared with WT plants with similarities to several changes observed in *ELTP::CDEF1* although more moderately (Fig. 4*D* and *SI Appendix*, Fig. S5*E* and Table S4). Among all these ionomic changes the levels of lithium, boron, sodium, calcium, manganese, arsenic, and strontium were found higher and the levels of phosphorous, nickel, and cadmium were found lower in both genotypes and could therefore be directly associated with an absence of endodermal suberin. On the other hand, *ELTP::MYB41* and *CASP1::MYB41* lines displayed more differences, with manganese, cobalt, nickel, copper, and cadmium accumulating in opposite manners (Fig. 4*D*). However, lithium and zinc accumulated at higher levels and boron, sodium, magnesium, phosphorous, potassium, calcium, iron, arsenic, rubidium, and strontium accumulated at lower levels in both *ELTP::MYB41* and *CASP1::MYB41* lines. To identify elements potentially directly affected by suberin among all these changes, we selected the elements commonly affected in the suberin-deficient *quad-myb* and *ELTP::CDEF1* plants and oppositely, but commonly, affected in the enhanced suberin *ELTP::MYB41* and *CASP1::MYB41* plants. Following this rationale, we found only a few elements following this trend with boron, sodium, calcium, arsenic, and strontium accumulating at higher levels in suberin-deficient plants and at lower levels in enhanced suberin plants (Fig. 4*D*). Importantly these ionomic changes were not explained by compensations in the expression of genes encoding transporters (*SI Appendix*, Fig. S5*F*). Among these elements, calcium and sodium were previously proposed to be directly affected by endodermal suberin and plants with reduced suberization were shown to accumulate these elements at higher levels (6, 11, 22, 46–48). In the context of sodium, endodermal suberin induction in response to salt stress was proposed to represent a protective mechanism against sodium entrance in plants. We set out to further test this hypothesis with the *quad-myb* mutant by studying its response to salt. First, we performed suberin staining on *quad-myb* treated with NaCl and observed that while this treatment induced suberization close to the root tip in WT plants as previously described (6), the *quad-myb* mutant was almost not responding (Fig. 4*E*). Next, we tested the tolerance of the *quad-myb* mutant to a mild salt treatment. When considering shoot weight and root length, *quad-myb* plants were significantly more reduced compared with WT plants when growing in the presence of salt (Fig. 4*F*) to degrees similar to what was described before for *ELTP::CDEF1* and the quintuple *gelp22-38-49-51-96* mutant (6, 43). Combined, our results further support the central role of suberin in plant adaptation to the presence of salt.

Discussion

Suberin plasticity in response to abiotic stresses such as drought, salt, waterlogging, or cadmium, while observed in roots in many species (20, 47–49), only recently started to be characterized at the molecular level. This topic gained increasing interest in the past few years after observing that endodermal suberin is even more plastic than previously thought, and not only overproduced in toxic environments but also tightly modulated in response to mineral deficiencies (6, 14, 21–25), to Casparian strip defects (9, 10, 12, 14, 16, 17), and during biotic interactions (25–28). In light of the plethora of signals controlling suberization, understanding the interaction between these pathways is critical. The potential interaction between ABA and SGN3/CIFs signaling has been previously interrogated (14, 36), suggesting complex coordination between SHR-dependent (SHORT ROOT) root development and ABA-mediated responses as well as between roots and shoots to control suberization. Here, we demonstrate by pharmacogenetic approaches that both pathways induce endodermal suberization independently (Fig. 1 and *SI Appendix*, Fig. S1). Corroborating our conclusion, a recent large-scale approach (combining microbiome, ionome, and suberin analysis, and genetics) revealed that the plant microbiome influences suberization through suppression of ABA-mediated signaling but independent of the SGN3/CIFs pathway (25).

In our attempt to identify transcription factors that are involved in ABA- and/or SGN3/CIFs-mediated suberization, we expected to identify specific factors downstream of at least one of these two pathways. We benefited from the impressive work performed by the community in identifying MYB transcription factors sufficient to induce suberization (29–33) and found four MYB transcription factors (*MYB41*, *MYB53*, *MYB92*, and *MYB93*) to be expressed in the endodermis at different degrees under unstressed conditions (Figs. 2*B* and *C* and 3 *C–E*). To our surprise all of them are induced in the endodermis in response to both ABA and CIF2 application with *MYB41* and *MYB93* being expressed close to the root tip after both treatment (Figs. 2*C* and 3 *C–E* and *SI Appendix*, Figs. S2 *C–G* and S3 *D–F*). This suggests that these four MYBs form a point of convergence between ABA and SGN3/CIFs signaling in the endodermis, with the signal specificity being established upstream of *MYB41*, *MYB53*, *MYB92*, and *MYB93*.

Confirming previous work in heterologous systems or whole-plant overexpression, we found that these four MYBs are sufficient to induce ectopic suberization when strongly expressed one by one in the endodermis prior to suberization (state I of endodermal differentiation) (Figs. 2 *D–G* and 3*B* and *SI Appendix*, Fig. S2*H*). Previous work showed in vitro that MYB41 can directly bind to the *LTP20* promoter (*LIPID TRANSFER PROTEIN20*, associated with functions in cutin and suberin export) (50) and MYB92 to the *BCCP2* promoter (*BIOTIN CARBOXYL CARRIER PROTEIN2*, involved in fatty acid synthesis) (33). Moreover, MYB53, MYB92, and MYB93 (as well as MYB9, MYB39, and MYB107) were shown in yeast one-hybrid and heterologous expression in tobacco leaves to activate the expression of *BCCP2* (33). In addition, MYB92 was shown to activate the expression of two other genes involved in fatty acid biosynthesis, *ACP1* (*ACYL CARRIER PROTEIN1*) and *LPD1* (*LIPOAMIDE DEHYDROGENASE1*) (33). Our analysis of conditional endodermal expression of *MYB41* showed that the expression of genes involved in suberin biosynthesis and polymerization is induced in roots shortly after MYB41 production (Fig. 2*G*). Additionally, we showed that endodermal accumulation of MYB41 protein can trigger the expression of the suberin biosynthesis gene *GPAT5* shortly after (Fig. 2*F* and *SI Appendix*, Fig. S2 *I* and *J*). Unfortunately, despite multiple attempts we were unable to immunodetect MYB41 protein from roots (either using the MYB41-Venus version described in this study or by attempts to raise an anti-MYB41 antibody), which would have allowed us to identify its direct targets in planta. This is probably due to working in its endogenous tissue (the late differentiated endodermis), which represents comparatively few cells of a whole root combined with a low abundance of MYB41, the protein accumulating only transiently in a few endodermal cells (Fig. 2*F* and *SI Appendix*, Fig. S2*J*). However, considering the high number of evidence from in vitro, yeast one-hybrid or transactivation assays in tobacco, we

can hypothesize that most suberin-inducing MYBs, including the four MYBs of interest in this study (MYB41, MYB53, MYB92, and MYB93), could directly activate the expression not only of genes involved in the primary fatty acid biosynthesis but also suberin biosynthesis genes in planta.

Loss of function of single suberin-inducing *MYB*s was rarely undertaken. Phenotypes were described only for *myb9* and *myb107* mutants, whose seed coats display a reduction in suberin monomers and an increased permeability, and for *myb39* mutant displaying a reduction of suberin monomers in whole roots but only a minor delay of a few cells in endodermal suberization (31, 40, 41). The mutants *myb41*, *myb53*, and *myb93* presented in this study, are not affected by suberin deposition in unstressed condition or in the presence of ABA or CIF2 (Fig. 3*A* and *SI Appendix*, Fig. S3*G*). Interestingly the single mutant *myb92* displayed a significant delay in suberin deposition in unstressed condition but its suberin was still strongly induced in response to ABA and CIF2 to levels similar to WT plants (Fig. 3*F*). We therefore took advantage of CRISPR-Cas9 gene editing to generate a quadruple *myb41-53-92-93* mutant (*quad-myb*). In nonstressed condition this *quad-myb* displayed a dramatic reduction of endodermal suberin with no suberin staining observed in endodermal cells and a reduction by 78% of suberin monomers detected in its roots (Fig. 4 *A* and *B* and *SI Appendix*, Fig. S4*C*). Mutants with such low amounts of endodermal suberin are extremely rare and most suberin biosynthesis mutants only moderately affect suberin amounts or its monomeric composition. For example, the *gpat5* mutant lacking a key enzyme for suberin biosynthesis displays only a 30% reduction of suberin monomer accumulating in its roots (51). To our knowledge, the only genotypes displaying a range of reduction comparable to the *quad-myb* is the quintuple *gelp22-38-49-51-96* mutant (affected in suberin polymerization in the cell wall), and the *ELTP::MYB4* line (where inhibition of the phenylpropanoid pathway in the endodermis leads to suberin detachment), both displaying an 85% reduction of suberin monomers in roots (43, 52). We are therefore confident that MYB41, MYB53, MYB92, and MYB93 are part of the core regulating machinery controlling suberization in the endodermis. However, the slight differences in their expression territories with only *MYB41*, *MYB53*, and *MYB92* expressed all along the suberizing zone and the suberin reduction observed in *myb92* but not in other single mutants suggest a certain level of specificity among these four *MYB*s in unstressed conditions (Figs. 2*C* and 3 *C–F* and *SI Appendix*, Fig. S2*C*). Importantly, in response to ABA or CIF2 the expression of all these *MYB*s was induced at different degrees, resulting in all of them being highly expressed close to the root tip and all along the endodermis (Figs. 2*C* and 3 *C–E* and *SI Appendix*, Figs. S2 *C–G* and S3 *D–F*). Moreover, testing the effect of ABA, salt stress (previously shown to be ABA dependent) (6), and CIF2, we found that suberin is virtually nonaffected by these three treatments in *quad-myb* (Fig. 4 *A* and *E* and *SI Appendix*, Fig. S4*C*). Yet, the fact that we could still observe in *quad-myb* a weak response (with few patches of suberized endodermal cells after ABA, salt, or CIF2 treatment) (Fig. 4*A* and *SI Appendix*, Fig. S4*C*), suggest that even more factors are either needed to fully regulate suberization or are not involved in suberization per se but capable of weakly compensating for the *quad-myb* defects. Such factors could be other endodermal *MYB*s (among which *MYB39* is an interesting candidate) with an endodermal expression induced by ABA and/or CIF2. Additionally, we could envision that other transcription factors such as bHLH transcription factors (basic helix–loop–helix) and/or a WD40-repeat protein (WD, tryptophan-aspartic acid) could influence endodermal suberization. It is known indeed that MYB-bHLH-WD40 protein complexes play central roles in controlling multiple cell fates such as root hair and trichome formation, anthocyanin biosynthesis, seed coat mucilage, or pigmentation (53–55).

As outlined in the introduction, suberin function for plant nutrition has recently benefited from the identification of mutants and lines affected in endodermal suberization and the wide application of ionomic analysis (6, 8–11, 13, 25, 31). However, even though all these studies are of fundamental interest to unravel suberin function and its physiological relevance, they are presently limited by the mutants and lines available at that time. In fact, plants with enhanced endodermal suberin, often characterized by their ionomic and physiological defects, are not specifically affected by this barrier. This is particularly the case for the enhanced suberin phenotypes being the consequence of Casparian strip defects, which activate SGN3/CIFs signaling and in turn lead to ectopic lignin and suberin deposition in the endodermis (9–12, 14, 16). In other words, the nutritional effect described in currently available analyses likely represent the consequence of multilevel defects in the endodermal barriers and of the activation of SGN3/CIF signaling. Because of these tissue-specific pleiotropic defects, the specific role played by suberin has remained unclear. On the other hand, mutants with a strong reduction of endodermal suberization were previously not available and studying a lack of suberin had been based on a synthetic line, artificially expressing a cutinase in the endodermis to degrade suberin (5, 6, 11, 14). While these lines showed a dramatic suberin reduction and were extremely important to distinguish between Casparian strip and suberin defects, we cannot exclude that artificially expressing the cutinase *CDEF1* in the endodermis would not lead to additional defects. Moreover, being highly plastic in response to nutrient availability (6, 14, 21–25), suberin defects described in nonstressed conditions can in some case be exacerbated or absent in stressed conditions (25). To fully understand suberin function in the endodermis we crucially need better and more specific mutants and lines with constitutively enhanced and reduced endodermal suberization. The lines presented here (*ELTP::MYB41* with constitutively enhanced suberization without any Casparian strip defects, and the *quad-myb* mutant with strongly reduced endodermal suberization and largely lacking regulation by ABA and salt stress) (Fig. 4 *A*, *B*, and *E* and *SI Appendix*, Fig. S4 *C–E* and *H*) provide such highly specific phenotypes. Their usefulness is highlighted by our ionomic analyses, which show clear differences between the enhanced suberin line *ELTP::MYB41*, a line combining enhanced suberin with Casparian strip defects (*CASP1::MYB41* line) and between the *quad-myb* and *ELTP::CDEF1* line (Fig. 4*D*). In summary our results suggest that, in accordance with previous reports, suberin plays crucial roles in nutrient homeostasis, likely directly affecting transport through the endodermis. But its role might be more specific than initially thought, affecting mainly the acquisition of boron, sodium, calcium, arsenic, and strontium in our experiments (Fig. 4*D*). We are therefore convinced that the tools generated in this study, especially the *quad-myb* and *ELTP::MYB41* plants will be of tremendous interest for the community in order to better understand suberin function in relation to nutrient availability as well as for its role in root development and biotic interactions. Given the increasing interest beyond fundamental research in manipulating suberin, extending the genetic tool box to specifically manipulate and fine tune suberization is highly relevant for applied plant biology in crop improvement or carbon capture to combat climate change.

Materials and Methods

Plant Material. All experiments were performed in Columbia-0 (Col-0) background. Previously published mutants and transgenic plants used in this study are as follows: *casp1-1 casp3-1*; *CASP1::NLS-GFP* (56); *esb1-1* (8); *sgn3-3*, *sgn3-4* (12); *ELTP::CDEF1*; *ELTP::NLS-3xmVenus* (6); and *myb92-2* (33). The mutants *myb53-1* (SALK_076713), *myb92-1* (SM_3.41690), and *myb93-1* (SALK_131752) were obtained from NASC (Nottingham Arabidopsis Stock Center). Primers used for genotyping are presented in *SI Appendix*, Table S1. Transgenic lines previously described and slightly modified in this study

are as follows: *ELTP::abi1-1* (based on ref. 4, here with a FastRed selection), *GPAT5::NLS-RFP* (based on *GPAT5::NLS-GFP* from ref. 5), and *GPAT5::mCitrine-SYP122* (6). The following mutants were generated for this study using CRISPR-Cas9 technology: *myb41_c1*, *myb41_c2*, *myb53_c1*, *myb93_c1*, and *myb41_c2-myb53_c1-myb92_c1-myb93_c1* (*quad-myb*, see constructs description in *SI Appendix* for more details). The following transgenic lines were generated for this study (construct described in *SI Appendix*): *MYB41::NLS-3xmVenus*, *MYB53::NLS-3xmVenus*, *MYB92::NLS-3xmVenus*, *MYB93::NLS-3xmVenus*, *GPAT5::NLS-3xmScarlet*, *CASP1xve::MYB41-mVenus*, *CASP1::MYB41*, *CASP1::MYB53*, *CASP1::MYB92*, *CASP1::MYB93*, *CASP1::myb41_c2*, *ELTP::MYB41*, *CASP1::myb53_c1*, *CASP1::myb92_c1*, and *CASP1::myb93_c1*. Growth conditions are described in *SI Appendix*.

Pharmacological Treatments. For 16-h treatments, seedlings were transferred on solid half-MS (Murashige and Skoog) media containing 1 μM ABA. For shorter treatments such as 3 h/6 h for staining, microscopy or gene expression analysis, a stock solution of ABA was diluted to 1 μM in liquid half-MS media applied directly onto roots without transfer of seedlings. The peptide CIF2, described in refs. 16, 19, was used at 1 μM and treatments were performed as described for the ABA treatment for short (3 h/6 h) and long (16 h) treatments. For 48-h fluridone treatments, 3-d-old seedlings were transferred on the half-MS containing 10 μM fluridone. Estradiol treatments were performed by diluting 5 mM of stock of estradiol to 5 μM in solid or liquid half-MS for long (16 h) and short (3 h/6 h) treatments, respectively.

Suberin Staining. Whole-mount suberin staining was performed as previously described in ref. 6. Five-day-old seedlings were incubated in FY 088 (0.01% wt/vol, lactic acid) for 30 min at 70 °C, washed twice with water, and then counterstained with Aniline Blue (0.5% wt/vol, water) for 30 min, washed with water, and mounted on glass slides to be observed with an epifluorescence stereomicroscope: Zeiss Axio Zoom.V16 with a GFP filter exitation (ex): 450 to 490 nm, emission (em): 500 to 550 nm. More details on image acquisition, analysis, and quantification are described in *SI Appendix*.

Confocal Microscopy. Confocal laser scanning microscopy experiments were performed either on a Zeiss LSM 780, a Zeiss LSM 800, or a Leica SP8 microscope. Excitation and detection windows were set as follows: Zeiss LSM 780: mVenus ex: 488 nm, em: 519 to 559 nm; RFP/mScarlet ex: 543 nm, em: 591 to 637 nm; Zeiss LSM 800: mCITRINE/mVenus ex: 488 nm, em: 500 to 546 nm; RFP/mScarlet ex: 561 nm, em: 585 to 617 nm; propidium iodide (PI) ex: 561 nm, em: 592 to 617 nm; and Leica SP8: Basic Fuchsin ex: 561 nm, em: 600 to 650 nm.

qRT-PCR. For gene expression analysis, 25 to 30 roots of 7-d-old seedlings were harvested and pooled together to form one biological replicate. RNA extractions were performed using a TRIzol-adapted RNeasy MinElute Cleanup Kit (Qiagen). RNA was reverse transcribed using a Thermo Scientific Maxima First Strand cDNA Synthesis Kit following the manufacturer's protocol. Real-time PCR was performed on an Applied Biosystems QuantStudio5 thermocycler using Applied Biosystems SYBR Green master mix. *ACTIN-2* (*At3g18780*) was used as the housekeeping gene and relative expression of each gene was calculated using the $2^{-\Delta\Delta Ct}$ method (57). The list of primer used for qRT-PCR are presented in *SI Appendix*, Table S2.

Chemical Suberin Analysis. We used the protocol described in ref. 58 for the analysis of ester-bound lipids, which likely belong only to suberin in the described organ and developmental stage. Analyses were performed from 5-d-old roots (between 200 and 300 per replicate, corresponding to 200 mg of seeds). More details are presented in *SI Appendix*.

Ionomic Analysis. Leaf elemental content was measured using ICP-MS as previously described (59). Nineteen elements were monitored (Li, B, Na, Mg, P, S, K, Ca, Mn, Fe, Co, Ni, Cu, Zn, As, Rb, Sr, Mo, and Cd). More details are provided in *SI Appendix*.

Statistical Analyses. Statistical analyses were done with GraphPad Prism 8.0 software (https://www.graphpad.com/) or with the R Environment (60). For statistical analysis of multiple transgenic lines, genotypes, or parametric or nonparametric treatments, one-way or two-way ANOVA and Tukey's test were used as multiple comparison procedures. Binary comparisons were performed using Student's *t* test.

Data Availability. All study data are included in the article and/or *SI Appendix*.

ACKNOWLEDGMENTS. We thank Robertas Ursache for sharing plasmids and methods for CRISPR-Cas9 mutagenesis and Lothar Kalmbach for destination plasmids allowing Fastgreen and Fastred selection after triple Gateway cloning and for critical reading of the manuscript. Owen Rowland and Dylan Kosma are thanked for sharing the MYB41 cDNA, Sébastien Baud for sharing *myb92-2* seeds, and Michael Hothorn for sharing CIF2 peptide. We thank Sylvain Loubéry and the Bioimaging Center at the University of Geneva for assistance with fluorescent microscopy and Rochus B. Franke for critical input on chemical analysis for suberin. We also thank Niko Geldner and his laboratory where preliminary work for this project was conducted. This work was supported by funding from the Sandoz Family Monique De Meuron philanthropic foundation's program for academic promotion and the Swiss National Science Foundation (Grant 31003A_179159 and Project Number PCEGP3_187007 to M.B. and Grants 310030_188672 and 31003A-170127 to C.N.), Max-Planck-Gesellschaft and the Sofia Kovalevskaya program from the Alexander von Humboldt foundation to T.G.A.

1. M. Barberon, The endodermis as a checkpoint for nutrients. *New Phytol.* **213**, 1604–1610 (2017).
2. P. Ramakrishna, M. Barberon, Polarized transport across root epithelia. *Curr. Opin. Plant Biol.* **52**, 23–29 (2019).
3. J. Alassimone, S. Naseer, N. Geldner, A developmental framework for endodermal differentiation and polarity. *Proc. Natl. Acad. Sci. U.S.A.* **107**, 5214–5219 (2010).
4. I. C. R. Barbosa, N. Rojas-Murcia, N. Geldner, The Casparian strip-one ring to bring cell biology to lignification? *Curr. Opin. Biotechnol.* **56**, 121–129 (2019).
5. S. Naseer *et al.*, Casparian strip diffusion barrier in Arabidopsis is made of a lignin polymer without suberin. *Proc. Natl. Acad. Sci. U.S.A.* **109**, 10101–10106 (2012).
6. M. Barberon *et al.*, Adaptation of root function by nutrient-induced plasticity of endodermal differentiation. *Cell* **164**, 447–459 (2016).
7. N. E. Robbins II, C. Trontin, L. Duan, J. R. Dinneny, Beyond the barrier: Communication in the root through the endodermis. *Plant Physiol.* **166**, 551–559 (2014).
8. I. Baxter *et al.*, Root suberin forms an extracellular barrier that affects water relations and mineral nutrition in Arabidopsis. *PLoS Genet.* **5**, e1000492 (2009).
9. P. S. Hosmani *et al.*, Dirigent domain-containing protein is part of the machinery required for formation of the lignin-based Casparian strip in the root. *Proc. Natl. Acad. Sci. U.S.A.* **110**, 14498–14503 (2013).
10. T. Kamiya *et al.*, The MYB36 transcription factor orchestrates Casparian strip formation. *Proc. Natl. Acad. Sci. U.S.A.* **112**, 10533–10538 (2015).
11. B. Li *et al.*, Role of LOTR1 in nutrient transport through organization of spatial distribution of root endodermal barriers. *Curr. Biol.* **27**, 758–765 (2017).
12. A. Pfister *et al.*, A receptor-like kinase mutant with absent endodermal diffusion barrier displays selective nutrient homeostasis defects. *eLife* **3**, e03115 (2014).
13. Z. Wang *et al.*, OsCASP1 is required for Casparian strip formation at endodermal cells of rice roots for selective uptake of mineral elements. *Plant Cell* **31**, 2636–2648 (2019).
14. P. Wang *et al.*, Surveillance of cell wall diffusion barrier integrity modulates water and solute transport in plants. *Sci. Rep.* **9**, 4227 (2019).
15. V. G. Doblas, N. Geldner, M. Barberon, The endodermis, a tightly controlled barrier for nutrients. *Curr. Opin. Plant Biol.* **39**, 136–143 (2017).
16. V. G. Doblas *et al.*, Root diffusion barrier control by a vasculature-derived peptide binding to the SGN3 receptor. *Science* **355**, 280–284 (2017).
17. S. Fujita *et al.*, SCHENGEN receptor module drives localized ROS production and lignification in plant roots. *EMBO J.* **39**, e103894 (2020).
18. T. Nakayama *et al.*, A peptide hormone required for Casparian strip diffusion barrier formation in Arabidopsis roots. *Science* **355**, 284–286 (2017).
19. S. Okuda *et al.*, Molecular mechanism for the recognition of sequence-divergent CIF peptides by the plant receptor kinases GSO1/SGN3 and GSO2. *Proc. Natl. Acad. Sci. U.S.A.* **117**, 2693–2703 (2020).
20. D. Líška, M. Martinka, J. Kohanová, A. Lux, Asymmetrical development of root endodermis and exodermis in reaction to abiotic stresses. *Ann. Bot.* **118**, 667–674 (2016).
21. A. Chen, S. Husted, D. E. Salt, J. K. Schjoerring, D. P. Persson, The intensity of manganese deficiency strongly affects root endodermal suberization and ion homeostasis. *Plant Physiol.* **181**, 729–742 (2019).
22. T. Knipfer, M. Danjou, C. Vionne, W. Fricke, Salt stress reduces root water uptake in barley (*Hordeum vulgare* L.) through modification of the transcellular transport path. *Plant Cell Environ.* **44**, 458–475 (2021).
23. J. Namyslov, Z. Bauriedlová, J. Janoušková, A. Soukup, E. Tylová, Exodermis and endodermis respond to nutrient deficiency in nutrient-specific and localized manner. *Plants* **9**, 201 (2020).
24. T. Armand, M. Cullen, F. Boiziot, L. Li, W. Fricke, Cortex cell hydraulic conductivity, endodermal apoplastic barriers and root hydraulics change in barley (*Hordeum vulgare* L.) in response to a low supply of N and P. *Ann. Bot.* **124**, 1091–1107 (2019).
25. I. Salas-González *et al.*, Coordination between microbiota and root endodermis supports plant mineral nutrient homeostasis. *Science* **371**, eabd0695 (2021).
26. J. Holbein *et al.*, Root endodermal barrier system contributes to defence against plant-parasitic cyst and root-knot nematodes. *Plant J.* **100**, 221–236 (2019).
27. A. Emonet *et al.*, Spatially restricted immune responses are required for maintaining root meristematic activity upon detection of bacteria. *Curr. Biol.* **31**, 1012–1028.e7 (2021).
28. C. Fröschel *et al.*, Plant roots employ cell-layer-specific programs to respond to pathogenic and beneficial microbes. *Cell Host Microbe* **29**, 299–310.e7 (2021).
29. D. K. Kosma *et al.*, AtMYB41 activates ectopic suberin synthesis and assembly in multiple plant species and cell types. *Plant J.* **80**, 216–229 (2014).

30. X. Wei *et al*., Three transcription activators of ABA signaling positively regulate suberin monomer synthesis by activating cytochrome P450 *CYP86A1* in kiwifruit. *Front Plant Sci* **10**, 1650 (2020).
31. H. Cohen, V. Fedyuk, C. Wang, S. Wu, A. Aharoni, SUBERMAN regulates developmental suberization of the Arabidopsis root endodermis. *Plant J.* **102**, 431–447 (2020).
32. K. Mahmood *et al*., Overexpression of ANAC046 promotes suberin biosynthesis in roots of *Arabidopsis thaliana*. *Int. J. Mol. Sci.* **20**, 6117 (2019).
33. A. To *et al*., AtMYB92 enhances fatty acid synthesis and suberin deposition in leaves of *Nicotiana benthamiana*. *Plant J.* **103**, 660–676 (2020).
34. D. J. Gibbs *et al*., AtMYB93 is a novel negative regulator of lateral root development in Arabidopsis. *New Phytol.* **203**, 1194–1207 (2014).
35. T. G. Andersen *et al*., Diffusible repression of cytokinin signalling produces endodermal symmetry and passage cells. *Nature* **555**, 529–533 (2018).
36. C. Wang *et al*., Developmental programs interact with abscisic acid to coordinate root suberization in Arabidopsis. *Plant J.* **104**, 241–251 (2020).
37. L. P. Popova, K. A. Riddle, Development and accumulation of ABA in fluridone-treated and drought-stressed *Vicia faba* plants under different light conditions. *Physiol. Plant.* **98**, 791–797 (1996).
38. C. R. Stewart, G. Voetberg, Abscisic acid accumulation is not required for proline accumulation in wilted leaves. *Plant Physiol.* **83**, 747–749 (1987).
39. N. Xu, J. D. Bewley, The role of abscisic acid in germination, storage protein synthesis and desiccation tolerance in alfalfa (*Medicago sativa* L.) seeds, as shown by inhibition of its synthesis by fluridone during development. *J. Exp. Bot.* **46**, 687–694 (1995).
40. J. Lashbrooke *et al*., MYB107 and MYB9 homologs regulate suberin deposition in angiosperms. *Plant Cell* **28**, 2097–2116 (2016).
41. M. Gou *et al*., The MYB107 transcription factor positively regulates suberin biosynthesis. *Plant Physiol.* **173**, 1045–1058 (2017).
42. H. Goda *et al*., The AtGenExpress hormone and chemical treatment data set: Experimental design, data evaluation, model data analysis and data access. *Plant J.* **55**, 526–542 (2008).
43. R. Ursache *et al*., GDSL-domain proteins have key roles in suberin polymerization and degradation. *Nat. Plants* **7**, 353–364 (2021).
44. R. Ursache, S. Fujita, V. D. Tendon, N. Geldner, Combined fluorescent seed selection and multiplex CRISPR/Cas9 assembly for fast generation of multiple Arabidopsis mutants. *bioRxiv* [Preprint] (2021). https://doi.org/10.1101/2021.05.20.444986. Accessed 21 May 2021.
45. D. K. Kosma, I. Molina, J. B. Ohlrogge, M. Pollard, Identification of an Arabidopsis fatty alcohol:caffeoyl-Coenzyme A acyltransferase required for the synthesis of alkyl hydroxycinnamates in root waxes. *Plant Physiol.* **160**, 237–248 (2012).
46. P. Krishnamurthy *et al*., Regulation of a cytochrome P450 gene *CYP94B1* by WRKY33 transcription factor controls apoplastic barrier formation in roots to confer salt tolerance. *Plant Physiol.* **184**, 2199–2215 (2020).
47. P. Krishnamurthy *et al*., The role of root apoplastic transport barriers in salt tolerance of rice (*Oryza sativa* L.). *Planta* **230**, 119–134 (2009).
48. P. Krishnamurthy, K. Ranathunge, S. Nayak, L. Schreiber, M. K. Mathew, Root apoplastic barriers block Na+ transport to shoots in rice (*Oryza sativa* L.). *J. Exp. Bot.* **62**, 4215–4228 (2011).
49. K. Shiono *et al*., RCN1/OsABCG5, an ATP-binding cassette (ABC) transporter, is required for hypodermal suberization of roots in rice (*Oryza sativa*). *Plant J.* **80**, 40–51 (2014).
50. M. H. Hoang *et al*., Phosphorylation by AtMPK6 is required for the biological function of AtMYB41 in Arabidopsis. *Biochem. Biophys. Res. Commun.* **422**, 181–186 (2012).
51. F. Beisson, Y. Li, G. Bonaventure, M. Pollard, J. B. Ohlrogge, The acyltransferase GPAT5 is required for the synthesis of suberin in seed coat and root of Arabidopsis. *Plant Cell* **19**, 351–368 (2007).
52. T. G. Andersen *et al*., Tissue-autonomous phenylpropanoid production Is essential for establishment of root barriers. *Curr. Biol.* **31**, 965–977.e5, 10.1016/j.cub.2020.11.070 (2021).
53. D. O. Robinson, A. H. K. Roeder, Themes and variations in cell type patterning in the plant epidermis. *Curr. Opin. Genet. Dev.* **32**, 55–65 (2015).
54. W. Xu, C. Dubos, L. Lepiniec, Transcriptional control of flavonoid biosynthesis by MYB-bHLH-WDR complexes. *Trends Plant Sci.* **20**, 176–185 (2015).
55. P. S. Millard, K. Weber, B. B. Kragelund, M. Burow, Specificity of MYB interactions relies on motifs in ordered and disordered contexts. *Nucleic Acids Res.* **47**, 9592–9608 (2019).
56. D. Roppolo *et al*., A novel protein family mediates Casparian strip formation in the endodermis. *Nature* **473**, 380–383 (2011).
57. K. J. Livak, T. D. Schmittgen, Analysis of relative gene expression data using real-time quantitative PCR and the 2(-Delta Delta C(T)) Method. *Methods* **25**, 402–408 (2001).
58. A. Berhin *et al*., The root cap cuticle: A cell wall structure for seedling establishment and lateral root formation. *Cell* **176**, 1367–1378.e8 (2019).
59. J. M. Danku, B. Lahner, E. Yakubova, D. E. Salt, Large-scale plant ionomics. *Methods Mol. Biol.* **953**, 255–276 (2013).
60. Team RC, R: A Language and Environment for Statistical Computing. R Foundation for Statistical Computing, Vienna, Austria. URL https://www.R-project.org/ (2019). Accessed 15 April 2021.